Limits on the WIMP-nucleon interactions with CsI(Tl) crystal detectors

H.S. Lee,[1] H.C. Bhang,[1] J.H. Choi,[1] H. Dao,[7] I.S. Hahn,[4] M.J. Hwang,[5] S.W. Jung,[2] W.G. Kang,[3] D.W. Kim,[1] H.J. Kim,[2] S.C. Kim,[1] S.K. Kim,[1,*] Y.D. Kim,[3] J.W. Kwak,[1,†] Y.J. Kwon,[5] J. Lee,[1,‡] J.H. Lee,[1] J.I. Lee,[3] M.J. Lee,[1] S.J. Lee,[1] J. Li,[7] X. Li,[7] Y.J. Li,[7] S.S. Myung,[1] S. Ryu,[1] J.H. So,[2] Q. Yue,[7] and J.J. Zhu[7]
(KIMS Collaboration)

[1]*DMRC and Department of Physics and Astronomy, Seoul National University, Seoul, Korea*
[2]*Department of Physics, Kyungpook National University, Daegu, Korea*
[3]*Department of Physics, Sejong University, Seoul, Korea*
[4]*Department of Science Education, Ewha Womans University, Seoul, Korea*
[5]*Department of Physics, Younsei University, Seoul, Korea*
[6]*Department of Engineering Physics, Tsinghua Universuty, Beijing, China*
[7]*Department of Engineering Physics, Tsinghua University, Beijing, China*

(Dated: February 5, 2008)

The Korea Invisible Mass Search (KIMS) experiment presents new limits on the WIMP-nucleon cross section using data from an exposure of 3409 kg·d taken with low-background CsI(Tl) crystals at Yangyang Underground Laboratory. The most stringent limit on the spin-dependent interaction for a pure proton case is obtained. The DAMA signal region for both spin-independent and spin-dependent interactions for the WIMP masses greater than 20 GeV/c^2 is excluded by the single experiment with crystal scintillators.

PACS numbers: 95.35.+d, 14.80.Ly

The existence of dark matter has been widely supported by many astronomical observations on various scales [1][2][3]. Weakly interacting massive particles (WIMPs) are a good candidate for dark matter well motivated by cosmology and supersymmetric models [4]. The Korea Invisible Mass Search (KIMS) experiment has developed low-background CsI(Tl) crystals to detect the signals from the elastic scattering of WIMP off the nucleus [5][6][7]. Both ^{133}Cs and ^{127}I are sensitive to the spin-independent (SI) and spin-dependent (SD) interactions of WIMPs. Recently, the role of CsI in the direct search for SD WIMP for pure proton coupling has been pointed out [8]. It is worth noting that ^{127}I is the dominant target for the SI interactions in the DAMA experiment. The pulse shape discrimination (PSD) technique allows us to statistically separate nuclear recoil (NR) signals of WIMP interactions from the electron recoil (ER) signals due to the gamma ray background [9][10].

The KIMS experiment is located at the Yangyang Underground Laboratory (Y2L) at a depth of 700 m under an earth overburden. Details of the KIMS experiment and the first limit with 237 kg·d exposure data can be found in the previous publication [11]. Four low-background CsI(Tl) crystals are installed in the Y2L and operated at a temperature of T = 0°C. Throughout the exposure period, the temperature of the detector was kept stable to within ±0.1°C. Green-enhanced photomultiplier tubes (PMTs) are mounted at both ends of each crystal. The signals from the PMTs are amplified and recorded by a 500 MHz FADC. Each event is recorded for a period of 32 μs. Both PMTs on each crystal must have at least two photoelectrons within a 2 μs window to form an event trigger. We obtained 3409 kg·d WIMP search data with four crystals, as shown in Table I. The energy is calibrated using 59.5 keV gamma rays from an ^{241}Am source. For calibration of the mean time, a variable used for the PSD, NR events are obtained with small crystals (3 cm × 3 cm × 3 cm) using an Am-Be neutron source. Compton scattering events taken with the WIMP search crystals using the ^{137}Cs source are used to determine the mean time distribution of the gamma background. Compton scattering events are also taken with the small crystals to verify that the mean time ditributions for both the test crystals and the WIMP search crystals are the same. In order to understand the nature of the PMT background, a dominant background at low energies, acrylic boxes are mounted on the same PMTs used for the crystals. The data obtained using this setup is used to develop the cuts for the rejection of PMT background.

TABLE I: Crystals used in this analysis and amount of data for each crystal

Crystal	mass (kg)	data (kg·days)
S0501A	8.7	1147
S0501B	8.7	1030
B0510A	8.7	616
B0510B	8.7	616
Total	34.8	3409

Since the decay time of the scintillation light in the CsI(Tl) crystal is rather long, photoelectrons are well separated at low energies and thereby enabling reconstruction of each photoelectron. The time distribution of photoelectrons in an event is fitted to a double exponen-

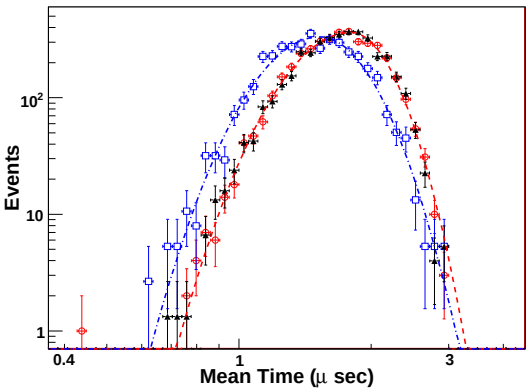

FIG. 1: (color online). MT distribution of NR events (open squares), ER events (open circles) and WIMP search data (filled triangles) of S0501A crystal in the 5-6 keV range. Fitted PDF functions are overlayed. χ^2/DOF =0.8 and 1.3 with DOF=38 and 35 for NR and ER events respectively.

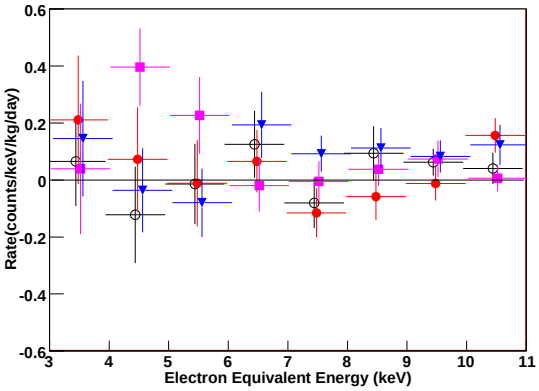

FIG. 2: (color online). Extracted NR event rates of the S0501A (open circles), S0501B (filled circles), B0510A (filled squares), and B05010B (filled triangles) crystals and only statistical errors (1σ) are shown. The points are shifted with respect to each other on the x-axis to avoid overlapping.

tial function given by

$$f(t) = \frac{1}{\tau_f}\exp\left\{\frac{-(t-t_0)}{\tau_f}\right\} + \frac{R}{\tau_s}\exp\left\{\frac{-(t-t_0)}{\tau_s}\right\},$$

where τ_f and τ_s are decay time constants of fast and slow components, respectively, R is ratio between two components, and t_0 is the time of the first photoelectron in the event. The mean time (MT) of each event is then calculated using these quantities as

$$MT = \int t\cdot f(t)dt / \int f(t)dt.$$

With this method, an improvement in PSD is achieved over the previous analysis where we used a simple mathematical mean [11]. In order to reject the PMT background, we applied cuts to the fit variable, τ_f. The ratio between the maximum log likelihood value of the double exponential fit and that of the single exponential fit is also used to reject the PMT background, since PMT background events tend to be shaped as single exponential decay. To reject the background that originates from the radioactivity of the PMT, the asymmetry between the signals from two PMTs is applied. Finally events in which signals are recorded in more than one crystal are rejected. The event selection efficiency was estimated by applying the same analysis cuts to the neutron and gamma calibration samples. The efficiency depends on the measured energy and ranges from 30% at 3 keV to 60% above 5 keV.

The estimation of the NR event rate is performed in each 1 keV bin from 3 to 11 keV for each crystal. The MT distributions of NR events and ER events are compared with the WIMP search data in Fig. 1 for the 5-6 keV energy range. The probability density functions (PDF) for the ER and NR events are obtained by fitting these distributions. An unbinned maximum likelihood fit is performed with the $log(MT)$ distribution of the WIMP search data using the likelihood function,

$$\mathcal{L}_i = \frac{1}{n!}\times\exp\{-(N_{NR,i}+N_{ER,i})\} \times\prod_{k=1}^{n}[N_{NR,i}PDF_{NR,i}(x_k)+N_{ER,i}PDF_{ER,i}(x_k)],$$

where the index i denotes the i-th energy bin; $n = N_{NR,i}+N_{ER,i}$ is the total number of events; $N_{NR,i}$ and $N_{ER,i}$ are the numbers of NR and ER events, respectively; $PDF_{NR,i}$ and $PDF_{ER,i}$ are PDFs of NR and ER events, respectively; and $x_k = \log(MT)$ for each event. The NR event rates obtained for each bin and for each crystal after efficiency correction are shown in Fig. 2. The extracted NR event rates are consistent with a null observation of the WIMP signal.

In order to obtain the expected measured energy spectrum of a WIMP signal including instrumental effects, a Monte Carlo (MC) simulation with GEANT4 [12] is used. A recoil energy spectrum is generated for each WIMP mass with the differential cross section, form factor, and quenching factor, as described in Ref. [13]. The spin-dependent form factor for ^{133}Cs calculated by Toivanen [14] is used, while for ^{127}I, Ressell and Dean's calculation [15] is used. The photons generated with the fitted decay function described above are propagated to the PMT and digitized in the same manner as in the experiment. Subsequently, the photoelectrons within given time windows are counted to check the trigger condition and to calculate energy. In this manner, the trigger efficieny and energy resolution is accounted for in the expected energy spectrum. The trigger efficiency is found to be higher than 99% above 3 keV. The simulation is verified with the energy spectrum obtained using 59.5 keV gamma rays from ^{241}Am. The peak position and

TABLE II: Spin expectation values for ^{133}Cs and ^{127}I

Isotope	J	$< S_p >$	$< S_n >$	Reference
^{133}Cs	7/2	-0.370	0.003	[16]
^{127}I	5/2	0.309	0.075	[15]

width of the distribution are very well reproduced for each crystal as described in Ref [11].

The total WIMP rate, R, for each WIMP mass is obtained by fitting the measured energy spectrum to the simulated one. The 90% confidence level (CL) limit on R is calculated by the Feldman-Cousins's approach in the case of Gaussian with a boundary at the origin [17] and then converted to the WIMP-nucleus cross section, σ_{W-A}. Subsequently, the limits on WIMP-nucleon cross section is obtained from Ref. [13][18] as follows:

$$\sigma_{W-n} = \sigma_{W-A}\frac{\mu_n^2}{\mu_A^2}\frac{C_n}{C_A},$$

where $\mu_{n,A}$ are the reduced masses of the WIMP-nucleon and WIMP-target nucleus of mass number A. $C_A/C_n = A^2$ for SI interactions and $C_A/C_n = 4/3\{a_p < S_p > +a_n < S_n >\}^2(J+1)/J$ for SD interactions. Here a_p, a_n are WIMP-proton and WIMP-neutron SD couplings respectively. The spin expectation values used for this analysis are shown in Table II. Following the "model-independent" framework [18], we report the allowed region in two cases for SD interaction: one for $a_n = 0$, and the other for $a_p = 0$. We express the WIMP-nucleon cross section as follows:

$$\sigma^{SI}_{W-n} = \sigma_{W-A}\frac{\mu_n^2}{\mu_A^2}\frac{1}{A^2},$$
$$\sigma^{SD}_{W-n,p} = \sigma_{W-A}\frac{\mu_{n,p}^2}{\mu_A^2}\frac{3}{4}\frac{J}{(J+1)}\frac{1}{< S_{n,p} >^2},$$

where we indicate pure proton (p, $a_n = 0$) and pure neutron (n, $a_p = 0$) coupling for SD interaction. We also present the allowed region in the $a_p - a_n$ plane with the following relation [18]:

$$\left(\frac{a_p}{\sqrt{\sigma_{W-p}}} \pm \frac{a_n}{\sqrt{\sigma_{W-n}}}\right)^2 \leq \frac{\pi}{24 G_F^2 \mu_p^2},$$

where G_F is the Fermi coupling constant.

The uncertainty in the MT distribution results in the uncertainty of the NR event rate. The limited statistics of the calibration data and different crystals used for the neutron calibration and WIMP search data are the major sources of this uncertainty. The former is investigated by varying the fitted parameters in PDF function within errors. The lattter is estimated by changing the mean of MT by the difference between the crystals. The systematic uncertainties from these two souces are combined in quadrature resulting in 20-30% of statistical uncertainties depending on the energy bins. In addition, there

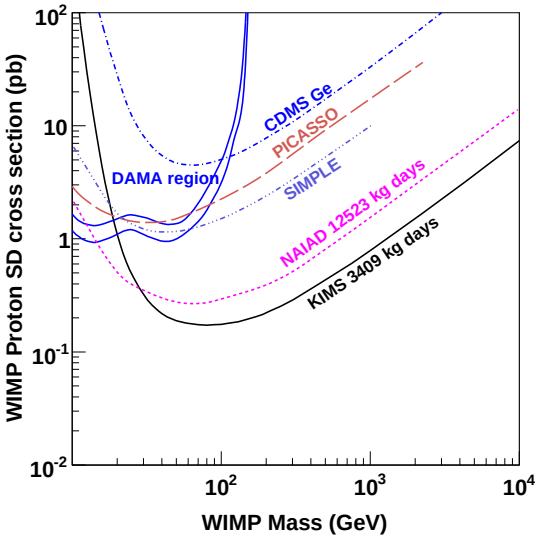

FIG. 3: (color online). Exclusion plot for the SD interaction in the case of pure proton coupling ($a_n = 0$) at the 90% confidence level

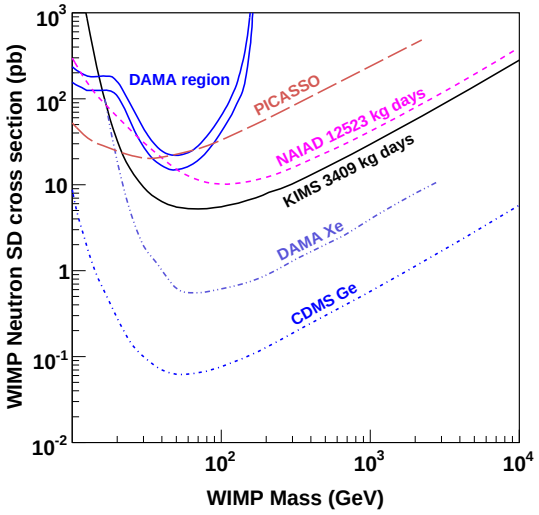

FIG. 4: (color online). Exclusion plot for for the SD interaction in the case of pure neutron coupling ($a_p = 0$) at the 90% confidence level

are uncertainties in the MC estimation of the expected event rates due to the uncertainties in the quenching factors and the difference of energy resolution between the MC simulation and the data. The systematic error from the MC simulation is estimated to be 13.3% of the limits. These systematic errors are combined with the statistical error in quadrature in the presented results.

The limits on the SD interactions are shown in Fig. 3 and 4 in the cases of pure proton coupling and pure neutron coupling, respectively. We also show the results obtained from CDMS [19], NAIAD [20], SIMPLE [21], and

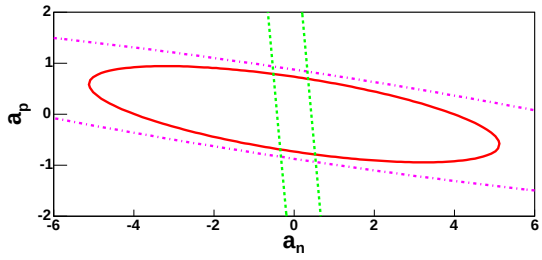

FIG. 5: (color online). Allowed region (90% confidence level) in $a_p - a_n$ plane by KIMS data (inside the solid line contour) for 50 GeV WIMP mass. Results of CDMS [19](dotted line) and NAIAD [20](dot-dashed line) are also shown.

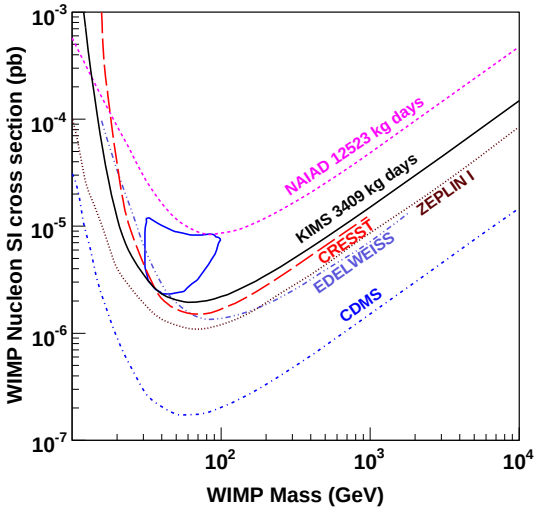

FIG. 6: (color online). Exclusion plot for the SI interactions at the 90% confidence level.

PICASSO [22]. The DAMA signal region is taken from Ref [23]. Our limit provides the lowest bound on the SD interactions in the case of pure proton coupling for a WIMP mass greater than 30 GeV/c^2. The allowed region in the $a_p - a_n$ plane for the WIMP mass of 50 GeV/c^2 is also shown in Fig. 5 together with the limits from CDMS and NAIAD. The limit for the SI interactions is shown in Fig. 6 together with the results of CDMS [24], EDELWEISS [25], CRESST [26], ZEPLIN I [27], and the 3σ signal region of DAMA (1-4) [28]. Although there are several experiments that reject the DAMA signal region, this is the first time that it is ruled out by a crystal detector containing ^{127}I, which is the dominant nucleus for the SI interactions in the NaI(Tl) crystal.

In summary, we report new limits on the WIMP-nucleon cross section with CsI(Tl) crystal detectors using 3409 kg·d exposure data. The DAMA signal regions for both SI and SD interactions are excluded for the WIMP masses higher than 20 GeV/c^2 by the single experiment. The most stringent limit on the SD interaction in the case of purely WIMP-proton coupling is obtained.

The authors thank Dr. J. Toivanen and M. Kortelainen for the calculation of the SD form factor as well as for the useful discussions. This work is supported by the Creative Research Initiative Program of the Korea Science and Engineering Foundation. We are grateful to the Korea Middland Power Co. Ltd. and the staff members of the YangYang Pumped Storage Power Plant for providing us the underground laboratory space.

* skkim@hep1.snu.ac.kr
† Current address: National Cancer Center, Ilsan, Korea
‡ Current address: Department of Physics, Ewha Womans University, Seoul, Korea

[1] K. G. Begeman, A. H. Broeils, and R. H. Sanders, Mon. Not. Roy. Astron. Soc. **249**, 523 (1991).
[2] D. N. Spergel et al., Astrophys. J. Suppl. **148**, 175 (2003).
[3] M. Tegmark et al., Phys. Rev. D **69**, 103501 (2004).
[4] G. Jungman, M. Kamionkowski, and K. Griest, Phys. Rep. **267**, 195 (1996).
[5] H. S. Lee et al., Nucl. Instr. Meth. A **571**, 644 (2007).
[6] Y. D. Kim et al., J. Korean. Phys. Soc. **40**, 520 (2002).
[7] Y. D. Kim et al., Nucl. Instr. Meth. A **552**, 456 (2005).
[8] T. A. Girard and F. Giuliani, Phys. Rev. D **75**, 043512 (2007).
[9] H. J. Kim et al., Nucl. Instr. Meth. A **457**, 471 (2001).
[10] H. Park et al., Nucl. Instr. Meth. A **491**, 460 (2002).
[11] H. S. Lee et al., Phys. Lett. B **633**, 201 (2006).
[12] S. Agostinelli et al., Nucl. Instr. Meth. A **506**, 250 (2003).
[13] J. D. Lewin and P. F. Smith, Astropart. Phys. **6**, 87 (1996).
[14] J. Toivanen and M. Kortelainen (2006), private communication.
[15] M. T. Ressell and D. J. Dean, Phys. Rev. C **56**, 535 (1997).
[16] F. Iachello, L.M.Krauss, and G. Maino, Phys. Lett. B **254**, 220 (1991).
[17] G. J. Feldman and R. D. Cousins, Phys. Rev. D **57**, 3873 (1998).
[18] D. R. Tovey et al., Phys. Lett. B **488**, 17 (2000).
[19] D. S. Akerib et al., Phys. Rev. D **73**, 011102 (2006).
[20] G. J. Alner et al., Phys. Lett. B **624**, 186 (2005).
[21] T. A. Girard et al., Phys. Lett. B **621**, 233 (2005).
[22] M. Barnabe-Heider et al., Phys. Lett. B **624**, 186 (2005).
[23] C. Savage, P. Gondolo, and K. Freese, Phys. Rev. D **70**, 123513 (2004).
[24] D. S. Akerib et al., Phys. Rev. Lett. **96**, 011302 (2006).
[25] V. Sanglard et al., Phys. Rev. D **71**, 122002 (2005).
[26] G. Angloher et al., Astropart. Phys. **23**, 325 (2005).
[27] G. J. Alner et al., Astropart. Phys. **23**, 444 (2005).
[28] R. Bernabei et al., Phys. Lett. B **480**, 23 (2000); R. Bernabei et al., Riv. Nuovo. Cim. **26**, 1 (2003).